# Next-to-leading order QCD corrections to the *Z* boson pair production at the LHC in Randall–Sundrum model

Neelima Agarwal [a], V. Ravindran [b], Vivek Kumar Tiwari [a], Anurag Tripathi [b],*

[a] *Department of Physics, University of Allahabad, Allahabad 211002, India*
[b] *Regional Centre for Accelerator-based Particle Physics, Harish-Chandra Research Institute, Chhatnag Road, Jhunsi, Allahabad 211019, India*

A B S T R A C T

The first results on next-to-leading order QCD corrections to production of two *Z* bosons in hadronic collisions in the extra dimension model of Randall and Sundrum are presented. Various kinematical distributions are obtained to order $\alpha_s$ in QCD by taking into account all the parton level subprocesses. We estimate the impact of the QCD corrections on various observables and find that they are significant. We also show the reduction in factorization scale uncertainty when $\mathcal{O}(\alpha_s)$ effects are included.

© 2010 Elsevier B.V. Open access under CC BY license.

## 1. Introduction

The last missing piece of the standard model (SM), the Higgs boson, remains elusive to this date, and it is hoped that the Large Hadron Collider (LHC) will shed light on the mechanism of spontaneous symmetry breaking and discover the Higgs bosons. Even if it is discovered there remain fundamental issues, such as the hierarchy problem and others, which make us believe in the existence of some new physics beyond the standard model. The LHC which will operate at an enormous centre of mass energy ($\sqrt{S} = 14$ TeV) promises to be a discovery machine and it is hoped that some signals of new physics beyond the SM will be observed. Extra

will consider the extra dimension model of Randall and Sundrum (RS) [3,4]. For a review of extra dimension models and their phenomenology see [5]. There are many important discovery channels at the LHC such as $\gamma\gamma$, $ZZ$, $W^+W^-$, jet production. In the SM the production of two *Z* bosons is suppressed as it begins at the order $e^4$ in the electromagnetic coupling and also because of the large $ZZ$ production threshold. The two *Z* bosons can couple to Kaluza–Klein (*KK*) gravitons, thus $ZZ$ pairs can be produced through virtual graviton exchange at the leading order. These ob-

servations make $ZZ$ production one of the important discovery channels.

At hadron colliders Quantum Chromodynamics (QCD) plays an important role as the *incoming* states in any scattering event are the partons, which are described by parton distribution functions (pdf's). The pdf's depend on the factorization scale ($\mu_F$) which is, to a large extent, arbitrary. This scale $\mu_F$ enters into any observable and makes it sensitive to the choice of its value and any leading order computation suffers from this sensitivity. However, as a computation beyond the leading order (LO) is carried out, the $\mu_F$ dependence partially cancels yielding results less sensitive to the factorization scale. It also improves upon LO results in that it includes a region which needs a treatment of the perturbation series. The organization of this Letter at the LHC at next-to-leading order (NLO) accuracy in the strong coupling constant in RS model.

Leading order studies for $ZZ$ production in the SM can be found in [6]. *Z* pair with a large transverse momentum jet at LO was studied in [7]. LO study for $ZZ$ production in the context of extra dimension model of RS was carried out in [8] and coupling of radion with gluon and top quark loop was considered in [9]. Because of its importance $ZZ$ production has also been studied to NLO accuracy in the SM [10–12]. These results were subsequently updated in [14,13]. NLO studies in SM via gluon fusion were carried out in [15,16]. These studies provide the precise estimate of higher order effects through *K* factor as well as the sensitivity of the predictions to factorization scale. Importantly, the corrections

* Corresponding author.
*E-mail addresses:* neel1dph@gmail.com (N. Agarwal), ravindra@hri.res.in (V. Ravindran), vivekkrt@gmail.com (V.K. Tiwari), anurag@hri.res.in (A. Tripathi).

turned out to be larger than the expectations based on soft gluon effects justifying a full-fledged NLO computation taking into all the processes. We presented NLO results for $ZZ$ production at the LHC in large extra dimension model of Arkani-Hamed, Dimopoulos and Dvali [1,2] in [17] where it was shown that the $K$ factors are large. The significance of NLO corrections in the Drell–Yan [18] and di-photon processes [19] in extra-dimension models has been already demonstrated. Although NLO results are available in SM and ADD model they do not exist in literature in the context of RS model which is the material of the present Letter.

The results which are presented in this Letter are obtained using our NLO Monte Carlo code (which is implemented on FORTRAN 77) that can easily accommodate any cuts on the final state particles and obtain various kinematical distributions. Our code is based on the method of two cutoff phase space slicing (for a review of the method see [20]) to deal with soft and collinear singularities in the real emission contributions. We will use the matrix elements presented in [17] and refer the reader to this Letter for further details.

In what follows we will first briefly describe the RS model and then present the numerical results and finally conclude.

## 2. RS model

The model of Randall and Sundrum addresses the hierarchy problem by introducing one extra spatial dimension which is compactified with a radius $R_c$ and is orbifolded. At the orbifold fixed point $\phi = \pi$ the Planck brane is located and the SM fields are localized at the TeV brane which is at $\phi = 0$. This geometry gives the following metric in 5-dimensions:

$$ds^2 = e^{-2\mathcal{K}R_c|\phi|}\eta_{\mu\nu}\,dx^\mu\,dx^\nu + R_c^2\,d\phi^2, \tag{1}$$

where $0 \leqslant \phi \leqslant \pi$. To explain the hierarchy between the Planck scale and the electroweak scale we need $\mathcal{K}R_c$ only of the order $\mathcal{O}(10)$. Introducing an extra scalar field in the bulk [21,22] showed that $\mathcal{K}R_c$ can me made stable against the quantum fluctuations.

The variations of the above setup have also been considered in the literature where the SM fields, except for the Higgs field, have been allowed to propagate in the bulk [23–27]. This framework provides an interesting new approach to the flavor problem, as now also the hierarchical structures observed in the masses and the mixing of the SM fermions could be explained in terms of geometrical effects [25,27–30]. In this Letter we will consider only the original proposal of Randall and Sundrum and carry out the NLO computation as the details of the QCD computation and the important results viz. $K$ factor, etc., will not depend on details of the realization of the RS model.

The effect of extra dimensions on the SM fields is felt through the $KK$ gravitons. These $KK$ gravitons, $h_{\mu\nu}^{(n)}$, couple to the SM energy–momentum tensor and the interaction Lagrangian is

$$\mathcal{L}_{int} \sim -\frac{1}{\overline{M}_{\text{Pl}}}T^{\mu\nu}(x)h_{\mu\nu}^{(0)}(x) - \frac{e^{\pi\mathcal{K}R_c}}{\overline{M}_{\text{Pl}}}\sum_{n=1}^{\infty}T^{\mu\nu}(x)h_{\mu\nu}^{(n)}(x). \tag{2}$$

$T^{\mu\nu}$ is the symmetric energy–momentum tensor for the SM particles on the 3-brane, and $\overline{M}_{\text{Pl}}$ is the reduced Planck scale. The masses of the $h_{\mu\nu}^{(n)}$ are given by

$$M_n = x_n \mathcal{K}\,e^{-\pi\mathcal{K}R_c}, \tag{3}$$

where the $x_n$ are the zeros of the Bessel function $J_1(x)$. The first term in the interaction Lagrangian gives the coupling of the zero-mode and it is Planck scale suppressed. The coupling of the massive $KK$ states is enhanced due to the exponential factor $e^{\pi\mathcal{K}R_c}$ and gives interactions of electroweak strength. Consequently, except for

the overall warp factor in the RS case, the Feynman rules in the RS model are the same as those for the ADD case [31,32]. The basic parameters of the RS model are

$$m_0 = \mathcal{K}e^{-\pi\mathcal{K}R_c},$$
$$c_0 = \mathcal{K}/\overline{M}_{\text{Pl}}, \tag{4}$$

where $m_0$ is a scale of the dimension of mass and $c_0$ ($0.01 \leqslant c_0 \leqslant 0.1$) is an effective coupling. For our analysis we choose to work with the RS parameters $c_0$ and $M_1$ the first excited mode of the graviton rather than $m_0$.

Summing over all the $KK$ states we obtain effective graviton propagator:

$$\mathcal{D}(Q^2) = \sum_{n=1}^{\infty}\frac{1}{Q^2 - M_n^2 + iM_n\Gamma_n} \equiv \frac{\lambda}{m_0^2}, \tag{5}$$

where $M_n$ are the masses of the individual resonances (see Eq. (3)) and the $\Gamma_n$ are the corresponding widths.

As the gravitons couple to $Z$ bosons, $PP \to ZZ$ can now also proceed through a process where gravitons appear at the propagator level. These new channels make it possible to observe deviations from SM predictions if extra dimensions exist. In the following we will consider spin-2 gravitons only at the propagator level and investigate this process at NLO level.

## 3. Numerical results

In this section we present invariant mass ($Q$) and rapidity ($Y$) distribution of the $Z$ boson pairs. These kinematical variables are defined as

$$Q^2 = (p_{Z_1} + p_{Z_2})^2, \qquad Y = \frac{1}{2}\ln\frac{P_1 \cdot q}{P_2 \cdot q}, \tag{6}$$

where $P_1$ and $P_2$ are the momenta of colliding hadrons, and $q = p_{Z_1} + p_{Z_2}$ denotes the sum of the $Z$-boson 4-momenta. In obtaining these distributions all order $\alpha_s$ contributions have been taken into account. At leading order in SM, the process proceeds through $q\bar{q}$ initiated process. As the gravitons couple to the $Z$ bosons, $q\bar{q}$ and $gg$ initiated processes with virtual gravitons also contribute at the same order in QCD. We have considered all the $q\bar{q}$, $gg$ initiated one loop virtual and, $q\bar{q}$, $qg$, $gg$ initiated real emission corrections to these processes, both in the SM and the gravity mediated processes, and their interferences. At the virtual level we used method of Passarino and Veltman [33] to reduce tensor loop integrals to scalar integrals. In dealing with real emission contributions we have used two cutoff phase space slicing method. Here, using two small dimensionless slicing parameters $\delta_s$ and $\delta_c$, the singular (soft and collinear) regions of phase space are separated from the finite hard noncollinear region. We will refer to the sum of contributions to cross section from virtual, soft and collinear regions as 2-*body* contribution, and from hard noncollinear region as 3-*body* contribution. The soft singularities cancel between real and virtual contributions and the collinear singularities were removed by mass factorization in $\overline{MS}$ scheme, this gives the finite 2-*body* contribution. Finally the kinematical distributions were obtained by integrating the 2-*body*, 3-*body* and leading order pieces over the phase space using Monte Carlo methods. Individually 2-*body* and 3-*body* contributions depend on the slicing parameters $\delta_s$ and $\delta_c$ but the sum is invariant against variations of these parameters over a wide range. For further analysis we will use $\delta_s = 10^{-3}$ and $\delta_c = 10^{-5}$. For further details please see [17].

Below we present various distributions for the LHC with a center of mass energy of 14 TeV as a default choice. However we will also present some results for a center of mass energy of 10 TeV
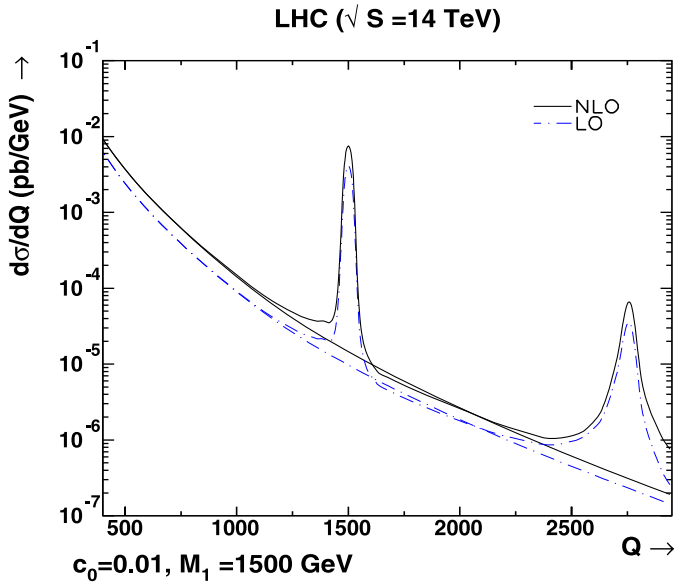
**Fig. 1.** Invariant mass distribution for SM and signal both at LO and NLO. Dash-dot curves represent LO results and solid curves give NLO results. We have chosen $M_1 = 1500$ GeV and the parameter $c_0 = 0.01$.



**Fig. 2.** Effect of variation of $c_0$ on invariant mass distribution. All the curves correspond to NLO results with $M_1$ fixed at 1500 GeV. The solid curve corresponds to SM and the dash-dot curves to the signal. The signal is plotted for $c_0 = 0.01, 0.04, 0.08$ and the dash size increases with increasing $c_0$.

for the LHC. For numerical evaluation, the following SM parameters [34] are used

$$M_Z = 91.1876 \text{ GeV}, \qquad \sin^2 \theta_W = 0.231 \tag{7}$$

where $\theta_W$ is the weak mixing angle. For the electromagnetic coupling constant $\alpha$ we use $\alpha^{-1} = 128.89$. CTEQ6 [35,36] density sets are used for parton distribution functions. 2-loop running for the strong coupling constant has been used, and we have done calculation with 5 quark flavors and taken the masses of quarks to be zero. The value of $\Lambda_{QCD}$ is chosen as prescribed by the CTEQ6 density sets. At leading order we use CTEQ 6L1 density set (which uses the LO running $\alpha_s$) with the corresponding $\Lambda_{QCD} = 165$ MeV. At NLO we use CTEQ 6M density set (which uses 2-loop running $\alpha_s$) with the $\Lambda_{QCD} = 22$ MeV; this value of $\Lambda_{QCD}$ enters into the evaluation of the 2-loop strong coupling. The default choice for the renormalization and factorization scale is the identification to the invariant mass of the $Z$ boson pair, i.e., $\mu_F = \mu_R = Q$. Furthermore the $Z$ bosons will be constrained to satisfy $|y_Z| < 2.5$, where $y_Z$ is the rapidity of a final state $Z$ boson.

In Fig. 1 we have plotted the invariant mass distribution both for the SM and the signal for LHC at 14 TeV. The two curves with peaks correspond to the signal and the remaining two curves give SM predictions. Here we have chosen $c_0 = 0.01$ and $M_1 = 1500$ GeV. To highlight the importance of QCD corrections we have also displayed the LO results of SM and the signal, and we observe that the $K$ factors (defined as $K = d\sigma^{NLO}/d\sigma^{LO}$) are large. For the signal the $K$ factor is 1.82 at $Q = 1500$ GeV. Next we present in Fig. 2 the effects of varying the parameter $c_0$ on the invariant mass distribution. All the curves shown correspond to NLO results, and we have also plotted the SM background for comparison.

In Fig. 3 we have plotted the rapidity distribution $d\sigma/dY$ at LO and NLO both for SM and the signal for $c_0 = 0.01$. We have carried out an integration over the invariant mass interval $1450 < Q < 1550$ to increase the signal over the SM background.

We have mentioned before that the NLO QCD corrections reduce the sensitivity of the cross sections to the factorization scale $\mu_F$; this we now show in Fig. 4. We have plotted SM and the signal both at LO and NLO, and have varied the factorization scale $\mu_F$ in the range $Q/2 < \mu_F < 2Q$. The central curve in a
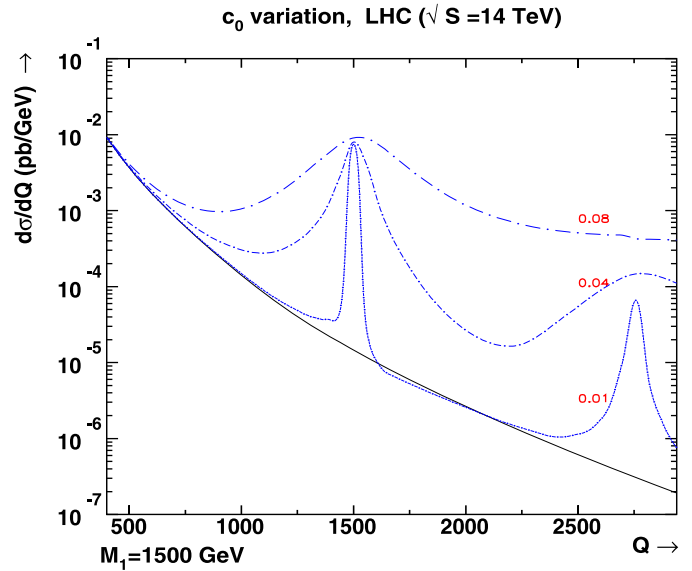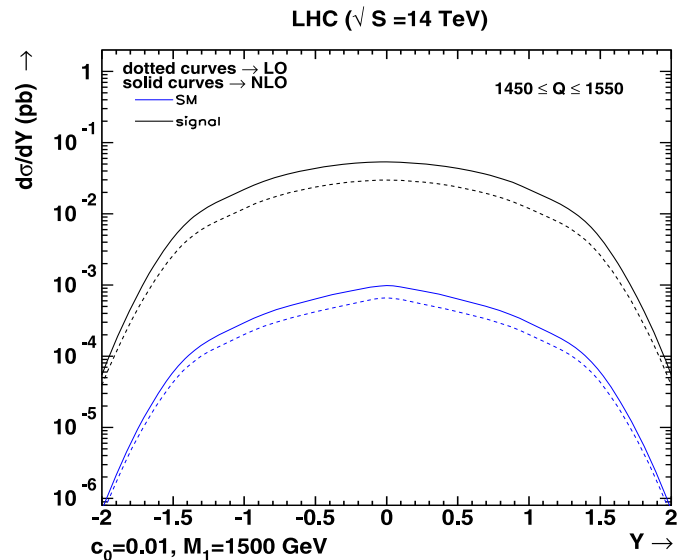


**Fig. 3.** Rapidity distribution for SM and signal both at LO and NLO. Dash curves represent LO results and solid curves give NLO results. We have chosen $M_1 = 1500$ GeV and the parameter $c_0 = 0.01$. To enhance the signal we have integrated over $Q$ in the range $1450 \leqslant Q \leqslant 1550$.

given band (shown by the dotted curves) correspond to $\mu_F = Q$. In all these results the renormalization scale is fixed at $\mu_R = Q$. We notice that the factorization scale uncertainty at NLO is much reduced compared to the LO. For instance at $Q = 1500$ GeV varying $\mu_F$ between $Q/2$ to $2Q$ shows a variation of 20.6% at LO for the signal, however the NLO result at the same $Q$ value shows a variation of 7.1%. Similarly we show the dependence on factorization scale at LO and NLO in the rapidity distribution in Figs. 5 and 6 for SM and signal respectively.

At the end we present in Fig. 7, $d\sigma/dQ$ for LHC with a centre of mass energy of 10 TeV at NLO both for SM and signal. For comparison we have also plotted the 14 TeV results in the same figure.
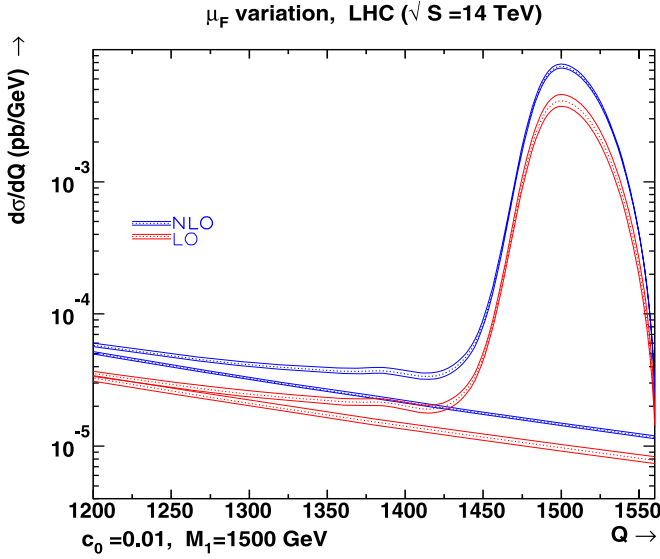
**Fig. 4.** Factorization scale variation in the invariant mass distribution. The curves correspond to $c_0 = 0.01$ and $M_1 = 1500$ GeV at the LHC at $\sqrt{S} = 14$ TeV. The $\mu_F$ is varied between $Q/2$ and $2Q$. The dash curves correspond to $\mu_F = Q$.
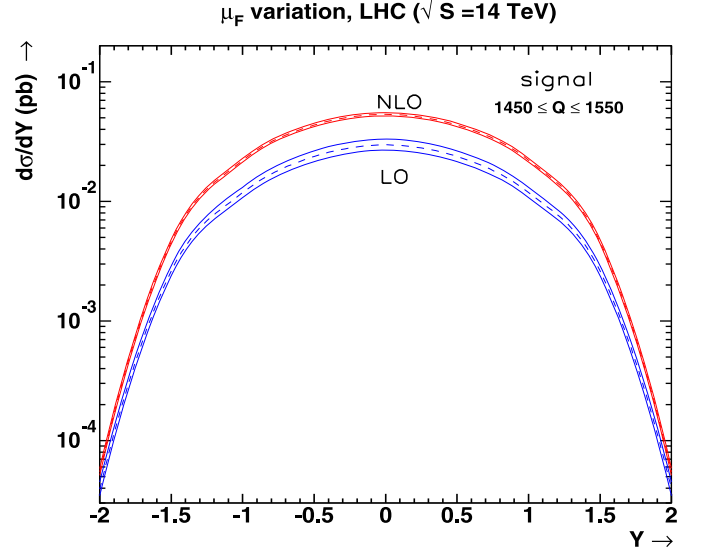


**Fig. 6.** Factorization scale variation in the rapidity distribution for signal. The curves correspond to $c_0 = 0.01$ and $M_1 = 1500$ GeV at the LHC at $\sqrt{S} = 14$ TeV. To enhance the signal we have integrated over $Q$ in the range $1450 \leqslant Q \leqslant 1550$. The $\mu_F$ is varied between $Q/2$ and $2Q$. The dash curves correspond to $\mu_F = Q$.
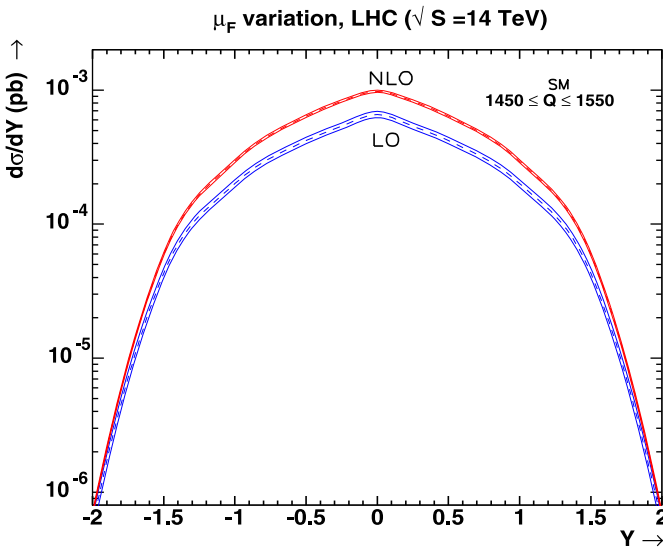


**Fig. 5.** Factorization scale variation in the rapidity distribution for the SM. We have integrated over $Q$ in the range $1450 \leqslant Q \leqslant 1550$. The $\mu_F$ is varied between $Q/2$ and $2Q$. The dash curves correspond to $\mu_F = Q$.



**Fig. 7.** Invariant mass distribution for SM and signal at $\sqrt{S} = 10$ TeV and 14 TeV. All the curves correspond to NLO results. We have chosen $M_1 = 1500$ GeV and the parameter $c_0 = 0.01$.

## 4. Conclusions

In this Letter we have carried out a full NLO QCD calculation for the production of two $Z$ bosons at the LHC at 14 TeV in the extra dimension model of Randall and Sundrum. Here we take all order $\alpha_s$ contributions, both in the SM and in the gravity mediated processes and their interferences, into account. We have presented invariant mass and rapidity distributions both at LO and NLO. We use CTEQ 6L1 and CTEQ 6M parton density sets for LO and NLO observables, respectively. Significant enhancements over the LO predictions are observed. The $K$ factors are found to be large, for instance in the invariant mass distribution the signal has a $K$ factor of 1.82 at $Q = 1500$ GeV (the position of first resonance). We have also presented the effects of variation of parameter $c_0$ both in $Q$ and $Y$ distributions. We have shown that a significant reduction in LO theoretical uncertainty, arising from
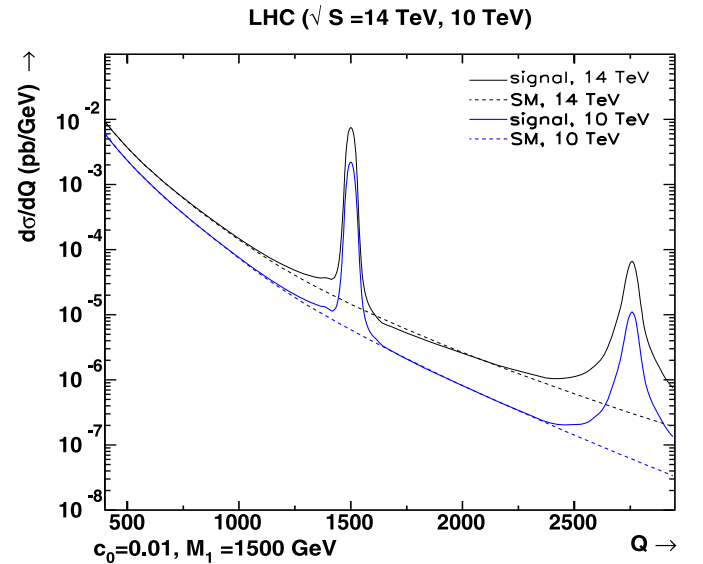
the factorization scale, is achieved by our NLO computation. For instance at 1500 GeV varying $\mu_F$ between $Q/2$ to $2Q$ shows a variation of 20.6% at LO for the signal, however the NLO result at the same $Q$ value shows a variation of 7.1%. Thus our NLO results are more precise than the LO results and suitable for further studies for constraining the parameters of the RS model. Invariant mass distribution is also presented for LHC at a center of mass energy of 10 TeV at the NLO level.

## Acknowledgements

## References

[1] I. Antoniadis, N. Arkani-Hamed, S. Dimopoulos, G.R. Dvali, Phys. Lett. B 436 (1998) 257, arXiv:hep-ph/9804398.
[2] N. Arkani-Hamed, S. Dimopoulos, G.R. Dvali, Phys. Lett. B 429 (1998) 263, arXiv:hep-ph/9803315.
[3] L. Randall, R. Sundrum, Phys. Rev. Lett. 83 (1999) 3370, arXiv:hep-ph/9905221.
[4] L. Randall, R. Sundrum, Phys. Rev. Lett. 83 (1999) 4690, arXiv:hep-th/9906064.
[5] K. Sridhar, Pramana 67 (2006) 607.
[6] R.W. Brown, K.O. Mikaelian, Phys. Rev. D 19 (1979) 922.
[7] U. Baur, E.W.N. Glover, J.J. van der Bij, Nucl. Phys. B 318 (1989) 106.
[8] S.C. Park, H.S. Song, J.H. Song, Phys. Rev. D 65 (2002) 075008, arXiv:hep-ph/0103308.
[9] P.K. Das, Phys. Rev. D 72 (2005) 055009, arXiv:hep-ph/0508103.
[10] J. Ohnemus, J.F. Owens, Phys. Rev. D 43 (1991) 3626.
[11] B. Mele, P. Nason, G. Ridolfi, Nucl. Phys. B 357 (1991) 409.
[12] B. Jager, C. Oleari, D. Zeppenfeld, Phys. Rev. D 73 (2006) 113006, arXiv:hep-ph/0604200.
[13] L.J. Dixon, Z. Kunszt, A. Signer, Phys. Rev. D 60 (1999) 114037, arXiv:hep-ph/9907305.
[14] J.M. Campbell, R.K. Ellis, Phys. Rev. D 60 (1999) 113006, arXiv:hep-ph/9905386.
[15] E.W.N. Glover, J.J. van der Bij, Nucl. Phys. B 321 (1989) 561.
[16] T. Binoth, N. Kauer, P. Mertsch, arXiv:0807.0024 [hep-ph].
[17] N. Agarwal, V. Ravindran, V.K. Tiwari, A. Tripathi, arXiv:0909.2651 [hep-ph].
[18] P. Mathews, V. Ravindran, K. Sridhar, W.L. van Neerven, Nucl. Phys. B 713 (2005) 333, arXiv:hep-ph/0411018;
P. Mathews, V. Ravindran, K. Sridhar, JHEP 0510 (2005) 031, arXiv:hep-ph/0506158;
P. Mathews, V. Ravindran, Nucl. Phys. B 753 (2006) 1, arXiv:hep-ph/0507250;

[19] M.C. Kumar, P. Mathews, V. Ravindran, Eur. Phys. J. C 49 (2007) 599, arXiv:hep-ph/0604135.
[19] M.C. Kumar, P. Mathews, V. Ravindran, A. Tripathi, Phys. Lett. B 672 (2009) 45, arXiv:0811.1670 [hep-ph];
M.C. Kumar, P. Mathews, V. Ravindran, A. Tripathi, Nucl. Phys. B 818 (2009) 28, arXiv:0902.4894 [hep-ph].
[20] B.W. Harris, J.F. Owens, Phys. Rev. D 65 (2002) 094032, arXiv:hep-ph/0102128.
[21] W.D. Goldberger, M.B. Wise, Phys. Rev. Lett. 83 (1999) 4922, arXiv:hep-ph/9907447;
W.D. Goldberger, M.B. Wise, Phys. Lett. B 475 (2000) 275, arXiv:hep-ph/9911457.
[22] C. Csaki, M. Graesser, L. Randall, J. Terning, Phys. Rev. D 62 (2000) 045015, arXiv:hep-ph/9911406;
C. Csaki, M.L. Graesser, G.D. Kribs, Phys. Rev. D 63 (2001) 065002, arXiv:hep-th/0008151.
[23] H. Davoudiasl, J.L. Hewett, T.G. Rizzo, Phys. Lett. B 473 (2000) 43, arXiv:hep-ph/9911262.
[24] A. Pomarol, Phys. Lett. B 486 (2000) 153, arXiv:hep-ph/9911294.
[25] Y. Grossman, M. Neubert, Phys. Lett. B 474 (2000) 361, arXiv:hep-ph/9912408.
[26] S. Chang, J. Hisano, H. Nakano, N. Okada, M. Yamaguchi, Phys. Rev. D 62 (2000) 084025, arXiv:hep-ph/9912498.
[27] T. Gherghetta, A. Pomarol, Nucl. Phys. B 586 (2000) 141, arXiv:hep-ph/0003129.
[28] N. Arkani-Hamed, M. Schmaltz, Phys. Rev. D 61 (2000) 033005, arXiv:hep-ph/9903417.
[29] S.J. Huber, Q. Shafi, Phys. Lett. B 498 (2001) 256, arXiv:hep-ph/0010195.
[30] S.J. Huber, Nucl. Phys. B 666 (2003) 269, arXiv:hep-ph/0303183.
[31] G.F. Giudice, R. Rattazzi, J.D. Wells, Nucl. Phys. B 544 (1999) 3, arXiv:hep-ph/9811291.
[32] T. Han, J.D. Lykken, R.J. Zhang, Phys. Rev. D 59 (1999) 105006, arXiv:hep-ph/9811350.
[33] G. Passarino, M.J.G. Veltman, Nucl. Phys. B 160 (1979) 151.
[34] C. Amsler, et al., Particle Data Group, Phys. Lett. B 667 (2008) 1.
[35] J. Pumplin, D.R. Stump, J. Huston, H.L. Lai, P.M. Nadolsky, W.K. Tung, JHEP 0207 (2002) 012, arXiv:hep-ph/0201195.
[36] D. Stump, J. Huston, J. Pumplin, W.K. Tung, H.L. Lai, S. Kuhlmann, J.F. Owens, JHEP 0310 (2003) 046, arXiv:hep-ph/0303013.